A Triptych of Plasma System Experiments

Cary Forest[1], Karsten McCollum[1], Ethan Peterson [1], Doug Endrizzi[1], Jay Anderson[1], Vladimir Mirnov[1], Bob Harvey[2], Justin Kasper[3], Stuart Bale[4], Carolyn Kuranz[3], Paul Drake[3]

[1]Physics Department, 1150 University Ave, University of Wisconsin-Madison, Madison, Wisconsin, 53706
[2] CompX
[3] University of Michigan
[4] University of California, Berkeley

(Received xx; revised xx; accepted xx)

During the past two years, a number of new heating and magnetic geometry capabilities have been added to the Big Red Ball device, allowing experiments that go beyond process-oriented research in experiments designed to create new laboratory plasma systems that evoke astrophysical geometries. A broad theme for experiments in this arena will be to understand the role of interfaces and boundary conditions, geometry and inhomogeneities, and how multiple processes interact. Here, we explore possible lessons to be learned from three proposed geometries that address system physics: (1) a Parker Spiral experiment investigating the interface between a flow-dominated and magnetically dominated plasma where magnetic fields are stretched and advected by a centrigully driven plasma wind, (2) a Space Weather experiment to study the system scale interfaces of a CME interacting with a magnetosphere, and (3) The creating of a CGL plasma in which a non-thermal component of fast particles modify MHD properties of a simple mirror plasma.

1. Introduction

The Big Red Ball (BRB) with its large size (diameter of 3 m) and unique confinement scheme using 0.4 T permanent magnets at the wall opens a door to the unexplored frontier of flow and pressure dominated plasma physics Forest *et al.* (2015). The base configuration facilitates super-Alfvénic flows to be induced at the plasma boundary under a large variety of plasma conditions ranging from well magnetized to completely unmagnetized. Furthermore, the BRB is built as two hemispheres which are separable (one hemisphere is on rails and the 3 ton structure can be moved by a single person). This allows for remarkable flexibility as structures such as interlocking internal coils can be prepared outside and then positioned inside the device using a 3 ton overhead crane. This flexibility has been recently used to create the TREX configuration where driven reconnection is studied under repeatable conditions and at magnetic Lundquist numbers unmatched by any other dedicated reconnection experiment. As a testament to its flexibility, the latest TREX configuration applies four 2 m diameter coils, which can be installed within a single work day. Other unique features of the BRB are the multiple methods by which plasmas can be produced and heated. These currently include combinations of RF-heating, Compact Toroid (CT) injections, LaB6 hot cathodes, arrays of plasma guns and inductive heating by internal coils. In short, given the unique features and base design of the experiment, the range of experimental configurations available in the BRB device is only limited by the user's imagination.

During the past two years, a number of new heating and magnetic geometry capabilities have been added to allow experiments that go beyond process-oriented research to create

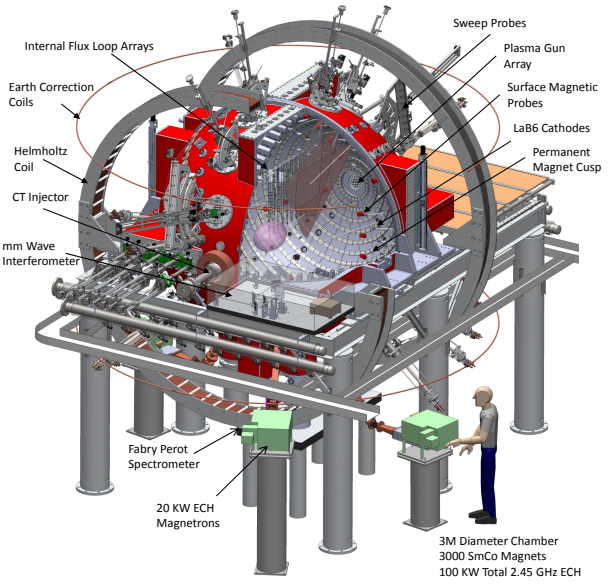

Figure 1: (color online) Overall Schematic of the BRB

new laboratory plasma systems that evoke astrophysical geometries. This allows building connections between fundamental processes and their interactions that are responsible for the self-organization of many astrophysical systems.

2. New Tools for The Big Red Ball

The **Big Red Ball** (Figs. 1) was built to create quasistationary flow and pressure dominated plasmas. It confines a large volume of unmagnetized plasma using a multi-cusp array of 0.4 T permanent magnets on the surface of a 3 m diameter sphere. The BRB is a large spherical multi-cusp device that was originally constructed as the Madison Plasma Dynamo Experiment with support for construction coming from the Major Research Instrumentation program of NSF. Its most unique feature is its capability to create and maintain flowing plasmas at high M_A with Rm and Re sufficiently high that dynamos should be possible. In addition to operating in both a dynamo scenario and in reconnection scenario, during the past year the device has explored a number of additional plasma formation techniques and novel geometries to further establish is potential for a User Facility.

The BRB device will gives Users great magnetic geometry flexibility. The 10 m^3 vacuum vessel itself uses 3000 Samarium Cobalt magnets bolted to its inner surface to provide multi-dipole surface confinement with a vanishing magnetic field in the core of the device. The magnets reduce the plasma loss area at the surface from the size of the vacuum vessel (10 m^2) to the linear dimension of rings times a width that is approximately an ion gyroradius (<0.2 m^2) thereby increasing the particle confinement ($\tau_p \sim 3$ ms) Cooper *et al.* (2017). The good confinement allows for plasma breakdown to occur at very low neutral pressures leading to a unique high ionization fraction, multi-dipole plasma. Many different sources have been demonstrated (as shown in Table 1).

In addition to the permanent magnets on the vessel surface, the experiment was constructed with a large Helmholtz coil (two additional planar electromagnets) outside

Plasma Source	Power	pulse	n_e $[10^{17}$ $m^{-3}]$	T_e $[eV]$	β	V	Re/Rm	$\mathcal{M}_f$ / $\mathcal{M}_\mathcal{A}$
ECH	100 kW	CW	0.5—5	1—10	0.01—50	—-	—	—
LaB_6 Cathodes	400 kW	CW	1—50	5—15	$> 10^4$	10 km/s	< 200 / < 200	0.5 / 10
Plasma Gun Array	2 MW	10 ms	1—50	5—15	$0.01—10^4$	20 km/s	5 / 2000	$1 / 0.1 - 10$
CT Pulsed Power	1 GW	10 μs	$50 - 100$	20	1	150 km/s	100 / 10^4	< 5 / < 5
TREX Pulsed Power	1 GW	100 μs	$50 - 100$	$20 - 40$	1	150 km/s	100 / 10^4	< 5 / < 5
NBI	1 MW	20 ms						

Table 1: Plasma Sources and heating systems available to WiPPL users.

the vessel that can be used to manipulate the large-scale field throughout the volume. These are water cooled, 5 meter diameter coils that can be used to apply a steady-state 400 gauss field to the entire sphere, either in a Helmholtz coil configuration or in a simple cusp configuration. Interestingly, this combination of surface confinement from the permanent magnets with an arbitrary large scale field makes it possible to access and control high temperature collisionless plasmas with arbitrary β.

Recently, the magnet geometries have been further augmented by three other types of magnets. The first is permanent magnet "magnetosphere" that can be immersed in the large background plasma atmosphere of the BRB. This simple SmCo cylindrical magnet has a diameter of 10 cm, and a net dipole moment of ***. The magnet is covered in an insulator, and electrodes have been installed in the upper and lower latitudes. The second is a set of very low inductance coils for applying fast changing magnetic fields to drive reconnection and shocks. The third is a set of higher field "mirror coils" installed at the ends of the device for controlling the shape of the large-scale field. Combined with the large Helmholtz field, these easily give a simple mirror. The strength of the mirror field does not need to be large since the multi-cusp magnets provide surface confinement. This allows for high β plasmas to be created using plasma guns in a non-paraxial (short/fat) mirror.

2.1. *Gun Plasmas*

An array of 19 plasma guns have been installed that allows 10 ms, high density and high temperature plasmas in a controlled way. Flux ropes can be created by driving current through the plasma.

2.2. *A CT injector for Shock Studies*

The observations and analysis of collisional shock waves in plasmas, including radiative shocks, in the context of HED research, are numerous. Collisionless shocks waves, in which the shock transition is produced by some sort of electromagnetic turbulence, have a long history in plasma physics, beginning with Sagdeev's prediction in the 1950's that the Earth produced a bow shock (Sagdeev 1966), leading over time to many space-based observations of such shocks. Biskamp (1973) reviews the laboratory observations

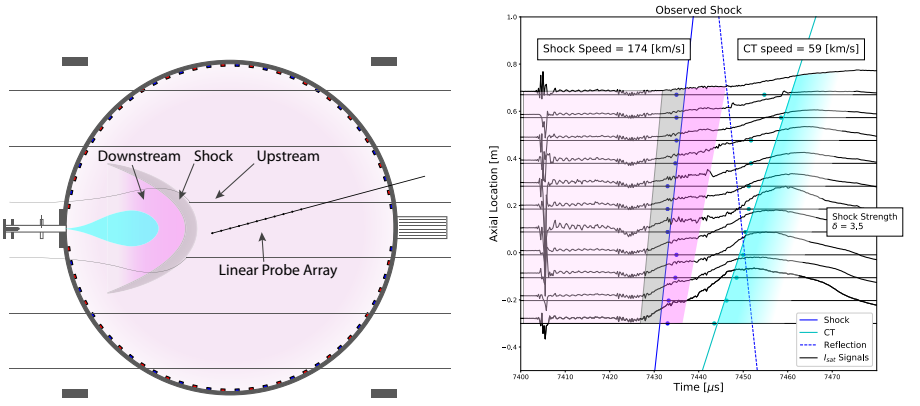

[h]

Figure 2: Shocks launched in the BRB. The schematic on the left shows application of a self-contained magnetized coaxial plasma gun (MCPG) system provided by Tri Alpha Energy Matsumoto *et al.* (2016). The MCPG is able to inject 100 MW of power for 10 μs to create a dense (10^{20} m^{-3}), fast (> 100 km s^{-1}) magnetized plasma slug (a compact toroid, or CT). Injecting this MCPG into large high β plasmas on the BRB is easy—the plasma creation and heating in the multi-cusp devise allows for uniform large plasmas with arbitrary magnetic fields that allow plasmas to have $\beta = 1 - \infty$. The speed of the CT is much faster than either a sound speed or an Alfvén speed: typical background plasmas have 5 eV, $10^{18} m^{-3}$, $B = 10$ gauss $c_s \sim V_A < 30$ km s^{-1}) and so the CT represents a Mach 4 supersonic piston and is expected to produce a shock. (Right) One plot showing Ion saturation measurements of n_e showing an apparent shock layer.

of collisionless shocks in the 1960s and 1970s, many of which were limited to shocks driven perpendicular to a magnetic field and all of which were hampered by the limited diagnostics of that era. Much later, Drake (2000) showed that modern lasers (and other devices that can propel dense enough matter at $\gtrsim 10$ kms^{-1}) could satisfy the constraints necessary to drive collisionless shocks that are relevant to astrophysics and space. Laboratory work eventually developed, and by now there have been studies of collisionless, quasi-perpendicular shocks (Niemann *et al.* 2014). Studies in counterstreaming, unmagnetized ion flows have included the transition from collisionless to collisional behavior (Moser & Hsu 2015), electrostatic shocks (Kuramitsu *et al.* 2011), and the Weibel instability (Fox *et al.* 2013; Huntington *et al.* 2015; Park *et al.* 2015). What has been missing until now is the ability to study parallel and quasi-parallel shocks with modern diagnostics, and to do so under conditions such that MHD effects are key to the shock dynamics, which is often the regime of shocks in space and astrophysics.

A diffuse, weakly magnetized plasma is an ideal target for the formation of magnetized parallel shocks. Recent compact toroid injection experiments on the BRB have demonstrated shock formation in front of a dense, high-velocity plasmoid impacting a background diffuse BRB plasma (see Fig. 2). The target plasma parameters can be adjusted to control the degree of collisionality and the angle of the shock with respect to the background field can be adjusted using external coils. Measurements of the particle distributions will expose both heating and energetic tail formation. In contrast with shock experiments carried out in HEDP experiments, the shock thickness is sufficiently macroscopic (~ 50 cm) that its substructure and dissipation mechanisms can be directly probed. Only a facility of sufficient scale can provide plasmas of sufficient size and density to probe shocks with a system scale of several c/ω_{pi}. Preliminary CT injection

experiments are already operating in an external user mode. Users will also include modelers who use high performance kinetic simulations to study astrophysical shocks. Such modeling applied to WiPPL plasmas will allow validation based on the combination of experimental and computational data.

3. Creating a Parker Spiral in the Lab

Field line stretching by plasma flow is the fundamental process that ultimately allows for magnetic fields to be created and perhaps the clearest example in nature of how flows can actively stretch and amplify magnetic fields is the magnetic Parker spiral create by the solar wind. Fig. **??** illustrates how the basic conditions for a centrifugally-driven wind in flow-dominated laboratory plasmas can be created in BRB.

The BRB's novel plasma stirring techniques use biased electrodes at the equator of the strong permanent dipole magnet to drive radial currents that in turn cause the plasma to rotate. This is essentially the same as the technique used to control the plasma flow on the boundary of the sphere but implemented in a magnetosphere geometry. Preliminary experiments together with numerical simulations of the geometry using NIMROD have established the feasibility of these experiments.

By creating such a system, we hope to model the magnetospheres rapidly rotating stars for which the rotation is so strong that the magnetic field can be centrifugally ejected. The NIMROD simulations show the formation of an equatorial current sheet and a magnetic Y-point where the dipole field breaks and is advected out into open field lines.

The plasma inhomogeneity in this geometry is a critical physics issue: near the dipole the plasma is magnetically dominated, while at large enough distances the plasma transitions to be flow-dominated. The interface defined by the position where the flow exceeds the Alfvén speed is known as an Alfvén radius in space and astrophysics. To the best of our knowledge this interface physics has never been studied in the lab. This interface can be considered the primary motivation behind the NASA Solar Probe+ mission, the first space mission to investigate the plasma near the Sun's Alfvén radius. Outside this Alfvén radius plasma inertia in the azimuthal and radial directions causes the magnetic field to pinwheel outward in a Parker spiral.

The major goals of this experiment would be:

(1)Measuring the equilibrium properties of a magnetically dominated rotating magnetosphere transitioning to a flow-dominated wind that advects magnetic field.

(2)Studying the stability of these rotating magnetospheres, paying special attention to rotationally driven instabilities like centrifugally driven interchange modes.

(3)Generate and observe reconnection and plasmoid formation in the resulting current sheet.

(4)Create a source of high-β turbulence driven by instabilities and reconnection.

Background: Stars and gaseous planets across the universe often exhibit two fundamental characteristics: dipolar magnetic fields and rotation. In the solar magnetosphere, this interplay between rotation and the magnetic field generates the Parker Spiral. Within a few solar radii, the strong magnetic field restricts coronal plasma to corotation with the solar surface. The $1/r^3$ dependence of the field strength means that further away from the sun, the kinetic energy of the solar wind dominates and field lines are stretched and dragged with the fluid flow. The location where the kinetic energy density and magnetic energy density are approximately equal is known as the Alfvén surface, R_A. Outside this surface, the radial outflow and azimuthal flow shear gives rise to the classic Archimedean spiral pattern **?**.

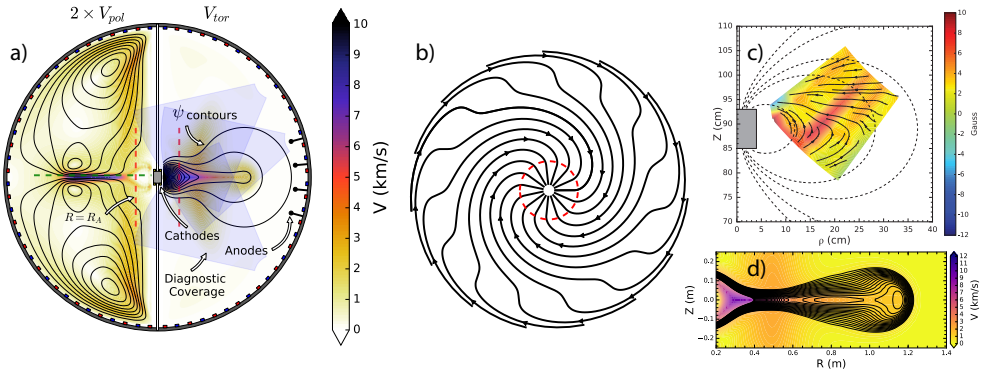

Figure 3: a) Experimental configuration for creating centrifugally driven wind and NIMROD Sovinec *et al.* (2004) MHD simulations of resulting flows and poloidal magnetic flux contours. Simulation parameters: $n_e = 6 \times 10^{17}\mathrm{m}^{-3}$, $T_e = 5$ eV, $T_i = 0.5$ eV, $Z_{eff} = 2$, which are well within achievable experimental bounds. At peak toroidal flow $S \approx 10$, $M_A \approx 5$, $Re \approx 375$. b) Magnetic field lines in R-φ plane from slice of NIMROD simulation along green dashed line in a) as seen from above with Alfvén radius R_A shown by red dashed circle. c) Prototype experiment demonstrating ability to generate real flows and advect poloidal magnetic field. d) NIMROD simulation with $T_e = 10$ eV exhibiting multiple X-line reconnection.

The solar Alfvén radius is typically between 10-30 solar radii and thus remains unexplored. The dynamics at this critical point are important to understanding the properties of the downstream solar wind, but physics at and below the Alfvén surface are often ignored in space weather forecasting models Sheeley Jr. (2017). The Solar Probe Plus mission, preparing to launch in 2018, will measure properties of the solar wind both above and below R_A on its journey down to 9.8 solar radii, providing invaluable data for improving forecasting models Guo *et al.* (2014). To complement this ground-breaking mission, experimental work like this proposal can provide predictions and insight into the character of the solar wind at the Alfvén surface.

Methodology: This experiment mimics the solar wind drive by replacing the thermal pressure force with a centrifugal force. A caveat is that the centrifugal drive has cylindrical as opposed to spherical symmetry; however, this difference should have little effect near the equator. Inserting the dipole magnet through the machine poles as displayed in Figure 3a will align the dipole moment, axis of rotation, and axis of symmetry while providing ample diagnostic access (shown by shaded wedges in Figure 3a). With the dipole in the center, it will be embedded in a large homogeneous unmagnetized plasma, ideally modelling the “infinite" extent of the heliosphere. Initial results from a prototype experiment were extremely promising and show advection of the poloidal field (Figure 3c) and measurement of toroidal flow in excellent qualitative agreement with the NIMROD simulations shown in Figure 3a,b. Figure 3 shows a picture of the SmCo dipole magnet central to the investigation. There are two fundamental configurations for this experiment, each with their own unique set of physics interests:

(1)**Radial Current Drive:** Biasing the polar electrodes with respect to electrodes in the bulk draws radial current. This current provides a $J \times B$ torque that will spin the magnetosphere, launching a radial wind outside the Alfvén surface. Quantifying and understanding hall effects in the magnetosphere will provide insight into the self-consistent solutions to the MHD equations, and how the solar wind transitions from the corotating region to the Parker Spiral. At the same time, we will be searching for dom-

[h]

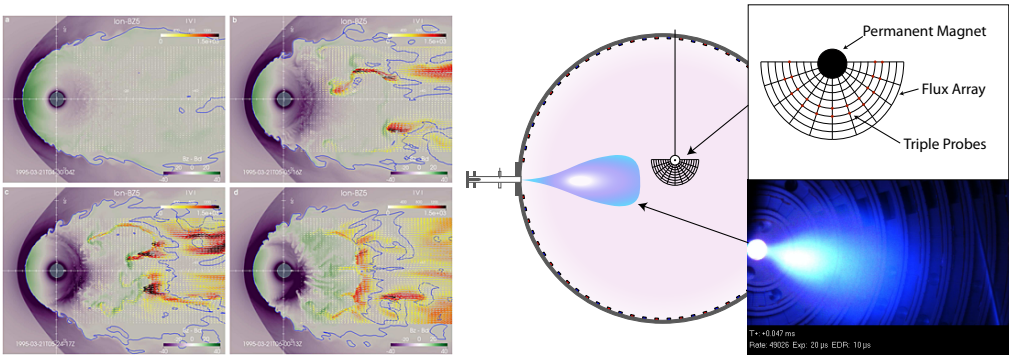

Figure 4: (Left) High resolution simulation performed by Wiltberger et. al. Wiltberger *et al.* (2015) depicting a BBF colliding with the Earth's magnetosphere. (Right) Experimental layout showing a still image of an injected CT and a mock up of the cylindrical flux array for measuring B_z, n_e and T_e.

inant transport mechanisms between the environmental plasma and the magnetosphere over a wide parameter space of rotation rates, density, and temperatures.

(2)**Pole to Pole Current Drive:** Driving current between the polar electrodes in a helicity injection scheme to launch flux rope like objects into the background plasma and observe their evolution. This configuration mimics a CME ejected from the surface of the Sun.

Plasma source and heating: Bulk plasma production will be from emissive LaB_6 cathodes and/or plasma guns as well as ECH, based on the desired density and temperature regimes of the background plasma. Current drive will be supplied by 100kW pulse forming networks or large capacitor banks used for reconnection experiments.

Equipment:

(i)Multi-tip mach/langmuir probe (existing)

(ii)3-axis hall probe array (existing)

(iii)SmCo dipole magnet and support (existing)

4. Space Weather

The major goals of this experiment would be to:

(1)Create and characterize a bow shock by colliding a supersonic plasma flow with a stationary magnetic field.

(2)Observe and characterize hydrodynamic instabilities that form and potentially transport plasma through a closed magnetic surface.

Background: Accurately forecasting space weather remains one of the most difficult challenges for future space travel and presently affects orbiting satellites, aircraft, communications, navigation, and power distribution Pulkkinen (2007). Key to understanding and accurately predicting potentially dangerous geomagnetic storms is the solar wind, a high β, supersonic, collisionless plasma that exhibits rapid changes in velocity, density, and field strength. Astronomers characterize some solar wind fluctuations as Bursty Bulk Flows (BBFs) and Interplanetary Coronal Mass Ejections (ICMEs). Typical BBFs and ICMEs have velocities that vary from 200 – 1000 km s^{-1}, densities around 4 – 10 cm^{-3} and field strengths of ∼10 nT when they encounter the Earth.

The Earth's bow shock forms when the ram pressure of the solar wind, $\sim \rho u^2$, where ρ is the mass density and u is the flow velocity, is equal to the Earth's magnetic field

pressure (or $\beta = 1$). The location of the bow shock can be predicted by equating these two pressures such that,

$$\frac{1}{2}\rho u^2 = \frac{1}{2\mu_0}(\mathrm{B}(\frac{\mathrm{r}_0}{\mathrm{r}})^3)^2, \tag{4.1}$$

and solving for r. Figure 4 (left) shows a simulation of a supersonic plasma (in this case, a BBF) colliding with the Earth's magnetic field and the formation of a bow shock. Many theories assume that the solar wind is in a steady state when, in fact, the density and velocity, and therefore the ram pressure, are highly variable. This results in the magnetosphere being a dynamic structure. In the laboratory we can characterize the dynamic pressure of the plasma flow and predict the standoff distance of the shock created when the flow collides with a magnetic field.

On the edges of the magnetosphere, the fast moving solar wind is adjacent to slower, denser magnetospheric plasma, creating a Kelvin-Helmholtz (KH) unstable region **??**. The resulting vortices can transport solar wind plasma into the magnetosphere, which causes geomagnetic storms. The simulations in Figure 4 (left) show developing structure that may be due to hydrodynamic instabilities. For low viscosity, incompressible flows, free of gravity and surface tension, the growth rate for the Kelvin Helmholtz instability is Chandrasekhar (1961):

$$\gamma_{ic} = \frac{k\Delta u}{2}\frac{\sqrt{\rho_1\rho_2}}{\rho_1+\rho_2}, \tag{4.2}$$

where k is the wavenumber of fluctuations at the interface between two fluids, the velocity difference across the interface is Δu, ρ is the density and the subscripts denote a specific fluid region. The compressibility of supersonic flows adds the correction factor Landau (1944),

$$\gamma = \gamma_{ic}\frac{\sqrt{-1-M_c^2+\sqrt{1+4M_c^2}}}{M_c}, \tag{4.3}$$

where M_c is the convective Mach number and $M_c = \Delta u/(c_1+c_2)$ with c being the speed of sound for a particular fluid. For the relatively low Mach number flows (4-5), the correction factor only slightly reduces the growth rate. By varying the dynamic pressure (i.e. the density and velocity) of the incoming flow we may be able to generate hydrodynamic instabilities in these flows.

Figure 4 (right) shows the layout for the initial proposed experiments, discussed further below. The magnetized coaxial plasma gun (MCPG) will fire a compact toroid (CT) or unmagnetized stream of plasma at a permanent dipole magnet. Once fully expanded, the CT densities drop to 10^{19} m^{-3} and velocities are $>$ 100 km s^{-1}. The permanent dipole magnet has a radius of $\sim$ 10 cm and a surface field of 3 kG. Solving for r when $\beta = 1$ gives an approximate location for the bow shock as 14 cm from the surface of the magnet. This is far enough from the surface of the magnet as to be easily measurable. Varying the velocity and density of the injected flow will alter the location of the bow shock.

Once a bow shock is experimentally observed, we can study the hydrodynamic instabilities generated as the fast-moving, injected plasma creates shear along the edges of the magnetized plasma. Initial estimates predict KH growth rates of $\sim$50 KHz. The typical CT crossing time is 40 μs so we will observe multiple growth rate periods of the KH instability. Varying the density and velocity of the injected flow will affect the KH growth.

Configuration: This experiment will use preexisting equipment repurposed from prior experiments. A strong ($\sim$ 3 kG permanent dipole magnet will be suspended in front of a MCPG provided by Tri Alpha. We can produce flows ranging from 50 to 200 km s^{-1}

with densities of $\sim 10^{13}$ cm^{-3} in a variety of gases (H_2, D_2, He, Ne, Ar), making high β, supersonic, moderately collisional plasmas. We will vary the injection velocity, density, and magnetization of the MCPG, which will vary the position of bow shock formation and KH growth.

5. Create a high β CGL plasma

A major long term goal for the field is the preparation of laboratory plasmas in which a turbulent cascade, dynamo, and small-scale kinetic instabilities (such as the mirror and firehose) are all active Schekochihin *et al.* (2005, 2008, 2009); Rosin *et al.* (2011). WiPPL heated plasmas provide this long-term possibility. This experiment has very demanding requirements; it needs to (1) be flow-dominated so that turbulence is actively stretching and amplifying magnetic field, (2) the plasma must have a sufficiently strong magnetic field that the ions are magnetized (able to execute many gyro-orbits during one collision time), and (3) the plasma pressure must be high compared to the magnetic pressure ($\beta \sim 1$) so that instabilities like mirror and firehose are unstable.

In the shorter term, WiPPL experiments can study how field-line stretching and amplification differs in very collisionless plasmas where anisotropic ion pressures are naturally produced through magnetic compression and rarefaction by flow in high-β (*pressure-dominated*) plasmas. We call this the CGL (Chew, Goldberger and Low) regime Chew *et al.* (1956) in which perpendicular and parallel pressures ($P_\perp$ and $P_\parallel$) have strong differences as a result of *e.g.* plasma flow shear driving anisotropy. One remarkable property of these plasmas is that the plasma motion can induce pressure anisotropy which exactly counteracts the induced magnetic tension, causing field lines to be much more easily distorted (flaccidity). To create the large plasma β and collisionless ions we propose to use a very simple mirror geometry implemented in the BRB (an intrinsically stable mirror plasma proposed by Ryutov Ryutov & Stupakov (1985)) to confine fast ions injected from the MST neutral beam heating system. Very anisotropic pressures are intrinsic to this plasma and the mirror and firehose instabilities will be investigated.

The major goals for this experiment would be as follows.

(1)The MHD stability of Ryutov's non-paraxial (spherical) mirror will be tested. Theory predicts MHD stability with $\beta \sim 1$.

(2)Create a highly anisotropic and collisionless fast ion population using MST's neutral beam heating system, injecting in to the BRB spherical mirror configuration.

(3)Observe firehose/mirror instabilities and/or ballooning modes; document change in V_A due to pressure anisotropy and thereby measure the flaccidity of the magnetic field.

Background: The ability to create a weakly collisional magnetized plasma in the laboratory opens a wealth of research opportunities at the frontier of plasma physics. In cosmic examples, these plasmas have a dynamical tendency to develop pressure anisotropies with respect to the local direction of the magnetic field which can trigger instabilities at scales just above the ion Larmor radius.Rosin *et al.* (2011); **?** Anisotropic pressure is a key feature in the dynamics of galaxy cluster plasmas, but is also relevant to Van Allen belt physics, solar wind and accretion flow plasmas**?**.

The magnetohydrodynamic (MHD) formulation of plasma equilibrium is an approximation to the Maxwell-Boltzman equations with expansion in small parameter λ_{mfp}/a (mean free path to system scale size) and ideal gas law closure. Isotropic pressure is maintained by frequent collisions**?**. When the mean free path is large (compared e.g. to ρ_L) the Chew-Goldberger-Low anisotropic solution**?** is appropriate. Expansion of Maxwell-Boltzmann is performed in small parameter ρ_L/a with a pressure tensor with

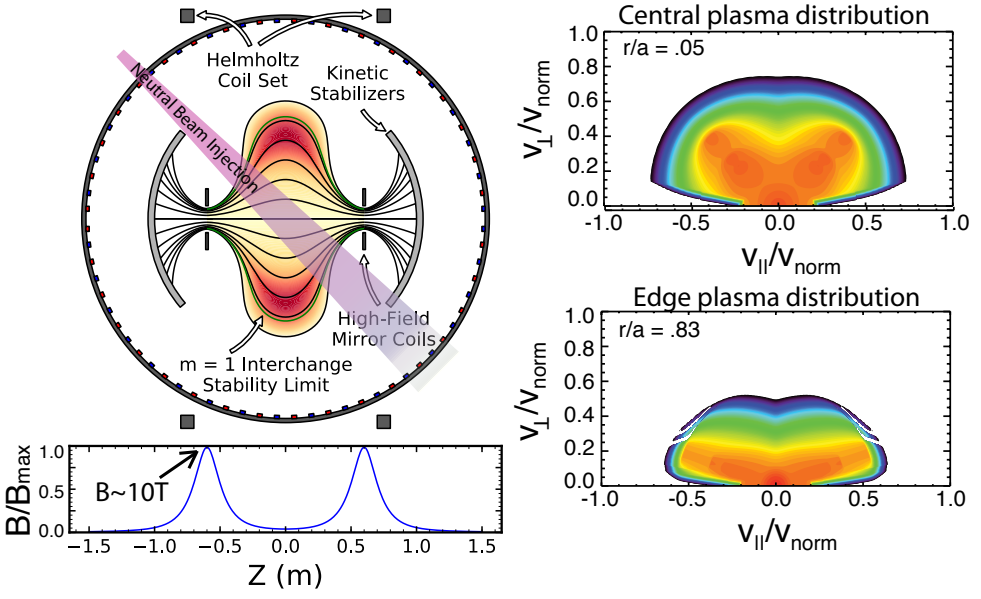

Figure 5: A nearly-collisionless, anisotropic laboratory plasma with $\beta \sim 1$ over a large volume can be created within the BRB device in a simple mirror geometry. High field superconducting mirror coils inside the device coupled with external Helmholtz coils create the non-paraxial mirror, with ECH for plasma formation and electron heating, and neutral beam injection for sourcing the anisotropic ion distribution.

two independent components (|| and $\perp$ to $\mathbf{B}$) and two equations of state are required for closure, $\frac{d}{dt}\left(\frac{p_\perp}{\rho B}\right) = 0$ and $\frac{d}{dt}\left(\frac{p_{||}B^2}{\rho^3}\right) = 0$.

We propose to create a laboratory plasma appropriately described by CGL equilibrium: collisionless ions at near-unity β over a large volume, by constructing a stable nonparaxial mirror configurationRyutov & Stupakov (1985) inside the BRB device. Two 10 Tesla REBCO coils are installed inside the spherical vacuum chamber, and combined with a pulsed power supply to the existing external Helmholtz coils, a mirror geometry is created with confining ratio $B_{max}/B_{min} \sim 200$. Plasma formation and heating is achieved with 100kW ECH and plasma gun array, and the anisotropic ion distribution is sourced by neutral beam injection. The magnetic field reconstruction is shown in Figure 5 along with ion distributions near the Z=0 equator, where parallel velocity is maximum and the tiny loss cone due to high mirror ratio is evident. There is good net curvature in the system, with the highest pressure at the turning points in a region of good curvature; the typical mirror 'bad' curvature near the radial boundary around Z=0 is a region of interest for studying global ballooning or other higher order modes (thought to be stabilized by FLR effects of the fast ion population).

In addition to the astrophysical examples above, more terrestrial plasma physics are accessible in this versatile configuration. Directed research will follow the construction phase, which of itself will be an accomplishment, being the first use of the REBCO high field superconductor to confine a hot plasma, and the first demonstration of the stable spherical mirror equilibrium. A first task is development of a proper equilibrium reconstruction with self-consistent treatment of anisotropic pressure using Fokker-Planck calculations of the ion distributions. Second, as diamagnetic reduction of the central field

increases the mirror ratio, with sufficient auxiliary heating spontaneous field reversal may occur in the central plasma. This will change the magnetic topology, presenting an O-point in the plasma for several studies, including the physics of fast ion current drive at an O-point**?**. Third, there are fascinating physics pertaining to the propagation of Alfvén waves as the phase speed is modified by a pressure anisotropy Rosin *et al.* (2011) $\omega = \pm k_{||}\left(\frac{p_\perp - p_{||}}{m_i n_i} + v_A^2\right)^{1/2} = \pm k_{||} c_s \left(\delta + \frac{2}{\beta}\right)^{1/2}$ where c_s is the sound speed and $\delta = \frac{p_\perp - p_{||}}{p_\perp}$. If the pressure anisotropy is such that $p_{||} > p_\perp$, the associated stress opposes the Maxwell stress (the magnetic tension force), the magnetic field lines become more easily deformable, and the Alfvén wave slows down. For a sufficiently parallel-dominated plasma (critical value of $\delta < -2/\beta$), the phase speed becomes zero and the Alfvén wave becomes a non-propagating unstable mode– the firehose instability. Correspondingly, the phase speed of the Alfvén wave will increase in our perpendicularly dominant plasma; the propagation characteristics can be measured by exciting the waves in a mirror geometry with a scheme recently performed in the LAPD.**?** Finally, the region of plasma near Z=0 and toward the radial boundary has a pressure gradient in the same direction as the local magnetic curvature; this presents an opportunity to study ballooning mode stability physics. These modes have been considered in studies of magnetospheric waves**?**, and, motivated by the fact that $p_\perp$ usually exceeds $p_{||}$ (particularly during magnetic storms**?**) Chan *et. al* **?** performed a theoretical analysis of the effects of anisotropic pressure on these modes. The predictions are that a ballooning-mirror stability threshold may exist at $p_\perp/p_{||} \gtrsim 2$. We can experimentally investigate the physics near this boundary with a beam injection angle scan and edge diagnostics tuned to look for the characteristic ballooning mode.

Methodology: Non-paraxial mirror on BRB

Plasma source and heating: Plasma guns, ECH, NBI, PPS (for driving Helmholtz coils).

Diagnostics: Routine diagnostics will include b-dot probes for stability, suite of fast ion diagnostics for distribution measurements, Langmuir and Hall probe arrays for equilibrium measurements.

This work was supported by U.S. Department of Energy Grant No. DE-SC0008708 and by National Science Foundation Grant No. 0903900. We wish to thank Hanto Ji, Jon Jara-Almonte, John Sarff, and Darren Craig for assistance in the design of the internal probe array and analog integrators.

REFERENCES

Biskamp, D. 1973 Collisionless shock waves in plasmas. *Nuclear Fusion* **13** (5), 719.

Chandrasekhar, S. 1961 *Hydrodynamic and Hydromagnetic Stability*. Oxford University Press.

Chew, G. F., Goldberger, M. L. & Low, F. E. 1956 The Boltzmanm equation and the one-fluid hydromagnetic equations in the absence of particle collisions. *Proc. Roy. Soc. A* **236**, 112.

Cooper, C.M., Weisberg, D., Khalzov, I., Flanagan, K., Milhone, J., Peterson, E., Wahl, C. & Forest, C.B. 2017 Direct measurement of the plasma leak-width in an optimized, high ionization fraction ring cusp—submitted. *Phys. Plasmas* **24**, 056502.

Drake, R. P. 2000 The design of laboratory experiments to produce collisionless shocks of cosmic relevance. *Physics of Plasmas* **7** (11), 4690–4698, arXiv: http://dx.doi.org/10.1063/1.1314625.

Forest, C B, Flanagan, K, Brookhart, M, Clark, M, Cooper, C M, Desangles, V, Egedal, J, Endrizzi, D, Khalzov, I V, Li, H, Miesch, M, Milhone, J, Nornberg,

M, Olson, J, Peterson, E, Roesler, F, Schekochihin, A, Schmitz, O, Siller, R, Spitkovsky, A, Stemo, A, Wallace, J, Weisberg, D & Zweibel, E 2015 The Wisconsin Plasma Astrophysics Laboratory. *Journal of Plasma Physics* **81** (05), 345810501–22.

Fox, W., Fiksel, G., Bhattacharjee, A., Chang, P.-Y., Germaschewski, K., Hu, S. X. & Nilson, P. M. 2013 Filamentation instability of counterstreaming laser-driven plasmas. *Phys. Rev. Lett.* **111**, 225002.

Guo, Yanping, McAdams, James, Ozimek, Martin & Shyong, Wen-Jong 2014 Solar probe plus mission design overview and mission profile.

Huntington, C. M., Fiuza, F., Ross, J. S., Zylstra, A. B., Drake, R. P., Froula, D. H., Gregori, G., Kugland, N. L., Kuranz, C. C., Levy, M. C., Li, C. K., Meinecke, J., Morita, T., Petrasso, R., Plechaty, C., Remington, B. A., Ryutov, D. D., Sakawa, Y., Spitkovsky, A., Takabe, H. & Park, H. S. 2015 Observation of magnetic field generation via the weibel instability in interpenetrating plasma flows. *Nature Phys.* **11** (2), 173–176.

Kuramitsu, Y., Sakawa, Y., Morita, T., Gregory, C. D., Waugh, J. N., Dono, S., Aoki, H., Tanji, H., Koenig, M., Woolsey, N. & Takabe, H. 2011 Time evolution of collisionless shock in counterstreaming laser-produced plasmas. *Phys. Rev. Lett.* **106**, 175002.

Landau, L. D. 1944 Stability of a tangential discontinuity in a compressible liquid. *Dokl. Akad. Nauk. SSSR* .

Matsumoto, T., Sekiguchi, J., Asai, T., Gota, H., Garate, E., Allfrey, I., Valentine, T., Morehouse, M., Roche, T., Kinley, J., Aefsky, S., Cordero, M., Waggoner, W., Binderbauer, M. & Tajima, T. 2016 Development of a magnetized coaxial plasma gun for compact toroid injection into the C-2 field-reversed configuration device. *Rev. Sci. Instrum.* **87**, 053512.

Moser, Auna L. & Hsu, Scott C. 2015 Experimental characterization of a transition from collisionless to collisional interaction between head-on-merging supersonic plasma jets. *Physics of Plasmas* **22** (5), 055707, arXiv: http://aip.scitation.org/doi/pdf/10.1063/1.4920955.

Niemann, C., Gekelman, W., Constantin, C. G., Everson, E. T., Schaeffer, D. B., Bondarenko, A. S., Clark, S. E., Winske, D., Vincena, S., Van Compernolle, B. & Pribyl, P. 2014 Observation of collisionless shocks in a large current-free laboratory plasma. *Geophysical Research Letters* **41** (21), 7413–7418.

Park, H.-S., Huntington, C. M., Fiuza, F., Drake, R. P., Froula, D. H., Gregori, G., Koenig, M., Kugland, N. L., Kuranz, C. C., Lamb, D. Q., Levy, M. C., Li, C. K., Meinecke, J., Morita, T., Petrasso, R. D., Pollock, B. B., Remington, B. A., Rinderknecht, H. G., Rosenberg, M., Ross, J. S., Ryutov, D. D., Sakawa, Y., Spitkovsky, A., Takabe, H., Turnbull, D. P., Tzeferacos, P., Weber, S. V. & Zylstra, A. B. 2015 Collisionless shock experiments with lasers and observation of weibel instabilities. *Phys. Plasmas* **22** (5), 056311, arXiv: http://aip.scitation.org/doi/pdf/10.1063/1.4920959.

Pulkkinen, Tuija 2007 Space weather: Terrestrial perspective. *Living Reviews in Solar Physics* **4** (1), 1.

Rosin, M.S., Schekochihin, A.A., Rincon, F. & Cowley, S.C. 2011 A non-linear theory of the parallel firehose and gyrothermal instabilities. *Mon. Not. Roy. Soc.* **413**, 7.

Ryutov, D. D. & Stupakov, G. V. 1985 Suppression of gross plasma instabilities in axisymmetric tandem mirrors. *Sov. J. Exp. Theor. Phys. Lett.* **42**, 35.

Sagdeev, R. Z. 1966 Cooperative phenomena and shock waves in collisionless plasmas. *Reviews of Plasma Physics* **4**, 23.

Schekochihin, A.A., Cowley, S.C., Kulsrud, R.M., Hammett, G.W. & Sharma, P. 2005 Plasma instabilities and magnetic field growth in clusters of galaxies. *Astrophys. J.* **629**, 139.

Schekochihin, A. A., Cowley, S. C., Dorland, W., Hammett, G. W., Howes, G. G., Quataert, E. & Tatsuno, T. 2009 Astrophysical Gyrokinetics: Kinetic and Fluid Turbulent Cascades in Magnetized Weakly Collisional Plasmas. *The Astrophysical Journal Supplement Series* **182** (1), 310.

Schekochihin, A. A., Cowley, S. C., Kulsrud, R. M., Rosin, M. S. & Heinemann, T.

2008 Nonlinear growth of firehose and mirror fluctuations in astrophysical plasmas. *Phys. Rev. Lett.* **100**, 081301.

Sheeley Jr., Neil R. 2017 Origin of the wang-sheeley-arge solar wind model. *Hist. Geo. Space Sci.* .

Sovinec, C. R., Glasser, A. H., Gianakon, T. A., Barnes, D. C., Nebel, R. A., Kruger, S. E., Schnack, D. D., Plimpton, S. J., Tarditi, A., Chu, M. & the NIMROD Team 2004 Nonlinear magnetohydrodynamics simulation using high-order finite elements. *J. Comput. Phys.* **195**, 355.

Wiltberger, M., Merkin, V., Lyon, J. G. & Ohtani, S. 2015 High-resolution global magnetohydrodynamic simulation of bursty bulk flows. *J. Geophys. Res.: Space Phys.* **120** (6), 4555–4566, 2015JA021080.